

## Designing Electroactive Biointerface for Spatiotemporal Control of Cell Attachment and Release

Sunny Shah<sup>a</sup>, He Zhu<sup>a</sup>, Jun Yan<sup>a</sup>, Stanislav Verkhoturov<sup>b</sup>, and Alexander Revzin<sup>a</sup>

<sup>a</sup>Department of Biomedical Engineering, University of California, Davis, Davis, California 95616, USA

<sup>b</sup>Department of Chemistry, Texas A & M University, College Station, Texas 77843, USA

In this paper, we demonstrate the use of individually addressable microelectrodes for cell sorting and cell micropatterning applications. Microelectrodes were modified with cell adhesive or non-adhesive molecules and then electrically stimulated to selectively adsorb or desorb proteins and/or mammalian cells. The switching of the surface properties was achieved by the electrochemical desorption of protein-functionalized thiols and poly(ethylene glycol) PEG silane from gold and indium tin oxide (ITO) electrodes respectively. The thiol surfaces were modified with anti-CD4 antibodies and used to capture T-cells. Upon electrical activation of the microelectrodes, both the antibodies and the T-cells were removed from the specific locations on the substrate. In addition, ITO electrodes were modified with cell-resistant PEG silane which was later electrochemically desorbed to make the surface adhesive to proteins or cells. This technique was employed to pattern two different cell types on the same substrate.

### Introduction

Electrical manipulation of interfacial properties has emerged as a method of exercising spatial and temporal control over protein- and cell-adhesive properties of the surface. Mrksich and co-workers developed alkanethiols that could be made cell-adhesive upon application of an oxidative potential to the underlying gold substrate and utilized this strategy to position two different cell populations on the same substrate (1). Recently, the same group developed a more complex strategy employing several alkanethiols, each possessing unique redox properties, to control attachment and release of cells from micropatterned substrates (2). These studies demonstrated an elegant approach to manipulate biointerfacial properties; however, the need to synthesize electroactive alkanethiols may confound the widespread use of this approach. In contrast, electrochemical desorption of alkanethiols offers a simple avenue for switching interfacial properties of gold substrates and has been used to control cell spreading from geometric confinements and to position three different cell types on the same surface (3-4). In addition to gold, indium tin oxide (ITO) has also been utilized to switch biointerfacial properties of the substrate. Gold and ITO are used as substrates due to their excellent conductivity and inertness. Studies by Voros and co-workers have employed custom-synthesized PEG-poly(L-lysine) (PLL) molecules that assembled on ITO through electrostatic interactions (5-6). The PEG-PLL layer was then desorbed by applying a positive potential.

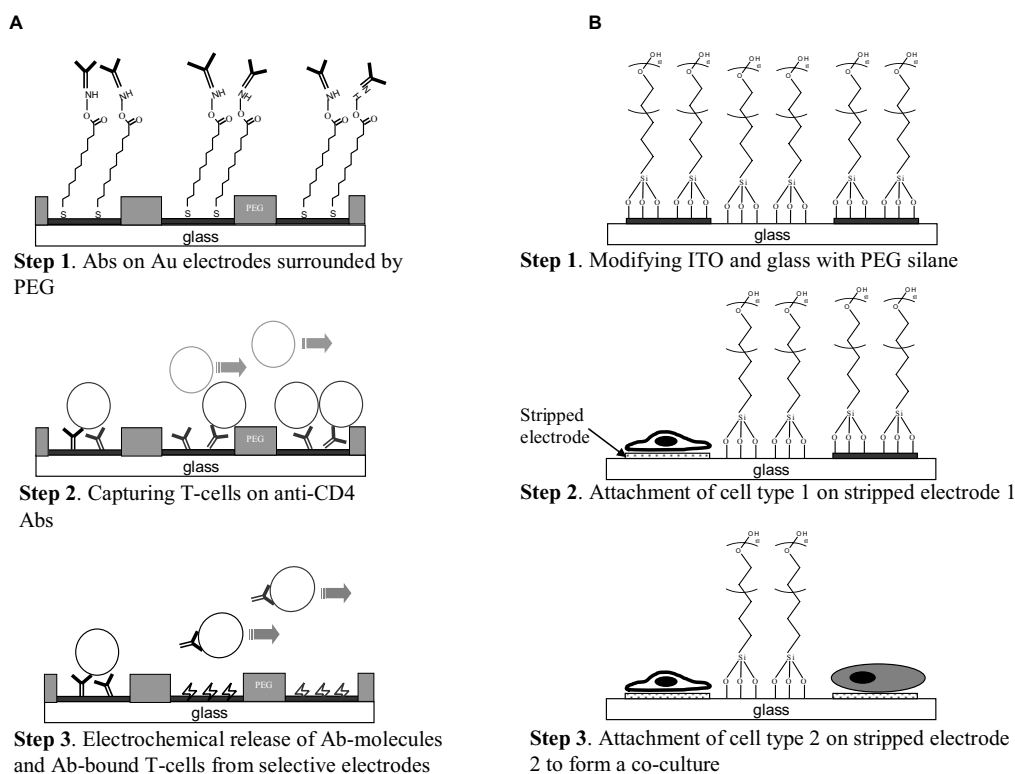


Figure 1: (A) Schematic for T-cell capture and release: Step 1: Covalent binding of anti-CD4 antibody molecules onto gold microelectrodes via COOH-terminated thiols. Step 2: Capture of T-cells exclusively onto Ab-modified gold microelectrodes. Step 3: Applying reductive potential ( $-1.2\text{V}$  vs. Ag/AgCl reference) disrupts the underlying thiol layer and results in release of T-cells. (B) Changing fouling properties of ITO substrates to pattern two cell types: Step 1: Modification of the ITO and surrounding glass substrate with non-fouling monolayer of PEG silane. Step 2: Application of reductive potential leading to desorption of PEG silane from a selective electrode followed by attachment of cell type 1. Step 3: Attachment of second cell type after activation of a second ITO electrode

In the present paper, electrochemical stimulation was used to release T-lymphocytes (T-cells) using an array of individually addressable gold electrodes (Figure 1A) (7). The T-cell release strategy employed here was based on electrochemical release of proteins from substrates described by us previously (8). Model T-cells expressing CD4 antigen were captured onto arrays of microelectrodes decorated with anti-CD4 Abs and packaged in PEG gel layer. Applying reductive potential ( $-1.2\text{V}$  vs. Ag/AgCl reference) to the desired electrode resulted in disruption of the underlying Ab layer and detachment of Ab-bound T-cells only from actuated members of an electrode array. Overall, fabrication of individually addressable Ab-modified microelectrodes provided a simple and effective means of releasing surface-bound T-cells with spatial and temporal control.

In a separate experiment, electrochemistry was used to pattern two distinct cell types on the surface (Figure 1B) (9). First, a glass substrate containing individually addressable ITO electrodes was modified with a non-fouling monolayer of PEG silane. A reductive potential ( $-1.4\text{V}$  vs. Ag/AgCl reference) lead to desorption of PEG silane

molecules from selective ITO electrodes. PEG silane desorption was characterized using time-of-flight secondary ion mass spectrometry (ToF-SIMS). Removal of PEG silane allowed attachment of cells and proteins. ITO substrates containing two individually addressable electrodes were used to assemble a co-culture of two distinct cell types. A sequence of PEG silane desorption and cell seeding steps were employed to form a co-culture of hepatic cells and fibroblasts. In the future, this technique can be utilized in the assembly of multiple cell types on the same substrate in a spatiotemporal fashion.

### Materials and Methods

Gold and ITO electrodes were fabricated using standard photolithography and wet etching techniques. ITO and gold substrates were dehydrated at 200 °C for 24 h prior to photoresist patterning. Positive photoresist (AZ5214-E) was spincoated on the substrates at 800 rpm for 10 s and 4000 rpm for 30 s. The substrate was then soft-baked at 100 °C for 105 s and exposed to UV light (10 mW/cm<sup>2</sup>) for 45 s. The exposed regions were developed for 5 minutes in AZ300 MIF developer solution, briefly washed with DI water and dried using nitrogen. Au-coated glass slides were immersed in Au etching solution (1:3, v/v mixture of Au-5 etchant with H<sub>2</sub>O) for 5 min, followed by 10 s immersion in Cr etching solution (1:1, v/v mixture of CR-4S etchant with H<sub>2</sub>O). ITO coated samples were placed in the ITO etchant comprising of 20% v/v hydrochloric acid, 5% v/v nitric acid, and 85% DI water. Remaining photoresist was removed from the ITO substrates by sonication in acetone for 20 minutes; however, photoresist was not removed from the gold substrates to protect the underlying Au during silane modification described below.

The glass substrates with gold electrodes were modified with 3-acryloxypropyl trichlorosilane (2 mM in anhydrous toluene). The substrates were then rinsed with fresh toluene, sonicated to remove the photoresist and baked at 100 °C for 3 h. Prepolymer solution, containing PEG-diacrylate (DA) (MW 575) and 2% (v/v) photoinitiator (2-hydroxy-2-methyl-propiophenone), was spincoated at 800 rpm for 4 s onto glass slides containing Au electrode patterns. PEG was polymerized on the glass regions using gold electrode as alignment marks. The substrate was flood-exposed from the back side with 365 nm, 5 mW/cm<sup>2</sup> UV light source for 40 s. The electrode surfaces were then decorated with Ab molecules using self-assembly of mercaptoundecanoic acid (MUA) followed by activation of –COOH end groups of this alkanethiol using EDC/NHS chemistry (8). Anti-human CD4 Ab solution (0.1 mg/ml in pH 4.5 sodium bicarbonate buffer) was reacted with activated MUA for 1 h. 50 nM Tris buffer was finally added to quench the remaining activated MUA. Reductive desorption of immobilized Abs was carried out in a custom-made Plexiglass electrochemical cell using a three electrode system. Micropatterned Au regions serving as working electrodes were enclosed inside an electrochemical cell, where 1× PBS served as an electrolyte solution. Ag/AgCl reference and Pt counter electrodes were positioned above the working electrode in the same volume. A potentiostat (CH Instruments, TX) was used to apply a reductive potential of (–1.2V vs. Ag/AgCl) for 60 s to individually addressable Au regions. Cyclic voltammetry, employing ferricyanide as a redox reporter molecule, was used to characterize electrode surface properties before and after disruption of the alkanethiol-Ab layer. Cyclic voltammetry was performed from 0 to 500mV (vs. Ag/AgCl) at a scan rate of 10 mV/s. Molt-3 cells were cultured in suspension in RPMI 1640 media with 10% (v/v) fetal bovine serum (FBS), 100 U/ml penicillin and 100 µg/ml streptomycin. The cells were spun down at 1200 rpm for 3 min and then re-suspended in 1x PBS to a final

concentration of  $5 \times 10^6$  cells/ml. The cells were incubated with the gold substrate decorated with antibodies for 15 minutes followed by a  $1 \times$  PBS wash to remove unattached cells. The desorption of T-cells using electrochemistry was carried out as described earlier.

For the ITO electrodes, the surfaces were modified with 2-methoxy(polyethylenoxy) propyltrichlorosilane for 2 h in anhydrous toluene (2% v/v) followed by a brief wash in fresh toluene. Modified substrates were baked at 100 °C for 2 h and stored in the desiccator until further use. Desorption of PEG silane was carried out in an electrochemical cell using the same setup described earlier; however, a voltage of -1.4V was applied for 60 seconds. Desorption of PEG silane from ITO was also examined by the SIMS method. The SIMS setup consisted of a custom-built  $C_{60}^+$  ion source coupled with ToF mass spectrometer.  $C_{60}^+$  ions were accelerated to +10 keV toward a negatively biased target (-5 keV), which resulted in a total impact energy of 15 keV.  $C_{60}^+$  projectiles impacting the target stimulated emission of secondary ions. The secondary ions were mass selected and detected by ToF mass spectrometer. The observations were made in the event-by-event bombardment-detection mode at the limit of single projectile impacts (super static regime of bombardment). Each spectrum was a summation of at least  $2 \times 10^6$  impact events over an impact area of  $10^{-2}$  mm<sup>2</sup>.

Hepatic cells (HepG2 cells) were maintained in MEM supplemented with 10% FBS, 200 U/mL penicillin, 200 µg/mL streptomycin, 1 mM sodium pyruvate, and 1 mM nonessential amino acids at 37 °C in a humidified 5% CO<sub>2</sub> atmosphere. Murine 3T3 fibroblasts were maintained in DMEM supplemented with 10% FBS, 200 U/mL penicillin, and 200 µg/mL streptomycin at 37 °C in a humidified 5% CO<sub>2</sub> atmosphere. To form the micropatterned co-culture, chosen ITO electrodes were activated to remove the underlying PEG silane layer. Upon incubation with 0.1 mg/mL collagen Type I solution, the protein adhered to the PEG silane desorbed region. Incubation of the substrate with HepG2 cells for 30 minutes formed cellular patterns corresponding to the electrode patterns. Prior to seeding the second cell type, HepG2 cells were allowed to spread out and occupy the electrode. To attach the fibroblasts, the second electrode was activated and the fibroblasts were seeded under similar conditions to form the co-culture. The samples were fixed in 4% paraformaldehyde solution and imaged using a Phillips XL30 scanning electron microscope.

## Results and Discussion

The present paper describes the development of a novel approach for releasing mammalian cells from microdevices. The cell release strategy was based on electrochemical disruption of an Ab layer bridging T-lymphocytes to the gold electrode surface. Adsorption and desorption of Ab layer was characterized by cyclic voltammetry with ferricyanide serving as a redox reporter molecule. Cyclic voltammetry allowed monitoring electron exchange across the electrode – ferricyanide solution interface as a function of biomolecular assembly occurring on the electrode surface. Figure 2A shows typical ferricyanide cyclic voltammograms collected from a single 300 µm diameter Au electrode. As seen from the data, bare Au electrode exhibited typical anodic and cathodic peaks associated with redox activity of ferricyanide. MUA self-assembly followed by Ab immobilization resulted in disappearance of the redox peaks, pointing to limited electron transfer across the electrode-solution interface (see Figure 2A). A number of studies

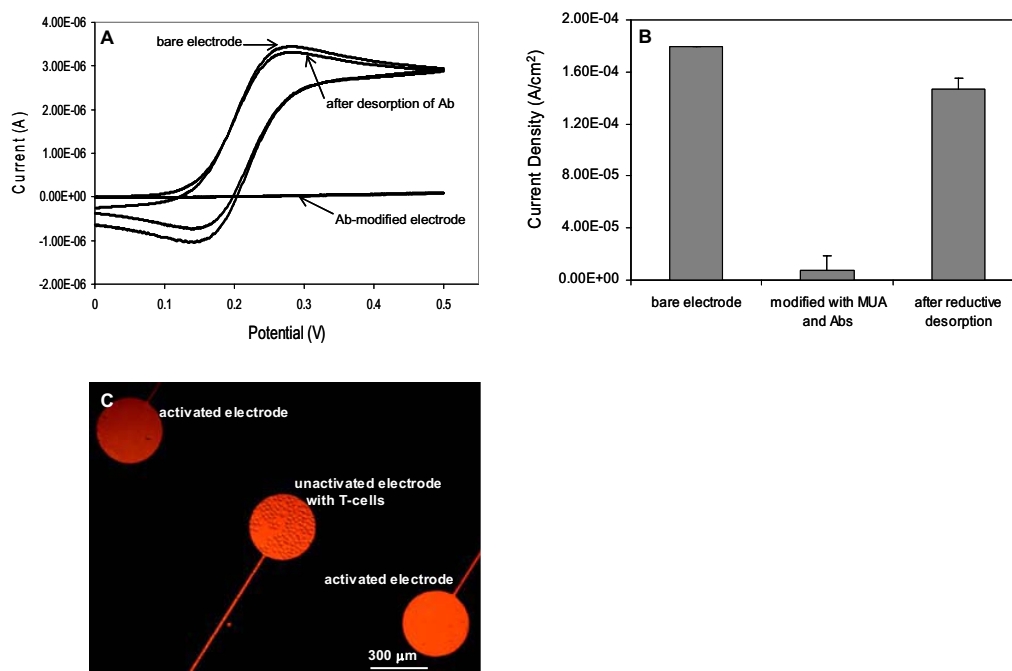


Figure 2: (A) Cyclic voltammetry of a single member of a microelectrode array (300  $\mu\text{m}$  diameter) performed at 10 mV/s in 5 mM ferricyanide solution. Application of reductive potential (-1.2V vs. Ag/AgCl) resulted in desorption of the alkanethiols-Ab layer and regeneration of cathodic and anodic peak typical of ferricyanide. (B) Anodic peak currents from ferricyanide cyclic voltammograms of four separate desorption experiments ( $n=4$ ). (C) An array of three individually addressable (300  $\mu\text{m}$  diameter) electrodes presented in the same field of view ( $\times 40$  magnification). Initially, T-lymphocytes were captured on all three electrodes, however, upper and lower electrodes were activated by applying reductive potential. The electrode in the center was not electrically activated. Trypan blue staining of T-lymphocytes released from the electrode surfaces revealed that  $\sim 90\%$  of cells were viable. Reproduced with permission from *Colloids and Surfaces B: Biointerfaces* **2008**, *64*, 260-268. Copyright 2008 Elsevier B.V.

reported reductive desorption of alkanethiols to occur in the potential range of -1 to -1.5V (3). In the present study, a potential of -1.2V (vs. Ag/AgCl reference) was applied for 60 s to effectively remove MUA and protein layers. Applying reductive potential to Ab-modified microelectrodes resulted in regeneration of anodic and cathodic redox peaks that were comparable in shape and magnitude to bare microelectrodes (Figure 2A). Figure 2B presents anodic peaks from ferricyanide cyclic voltammetry performed before and after reductive desorption experiments. As seen from these data, regeneration of the electron exchange across the electrolyte – electrode interface upon applying negative potential was highly repeatable. The electrochemistry experiments provided direct evidence of disruption and desorption of the passivating alkanethiol-Ab layer from the microelectrode surface.

T-lymphocytes are responsible for orchestrating adaptive immune response and, therefore, represent a particularly important subset of leukocytes. For example,  $\text{CD4}^+$  T-cells are preferentially destroyed by HIV/AIDS, resulting in compromised immunity and greatly increasing patients' susceptibility to opportunistic infections (10-11). The

diagnostic importance of leukocytes in general and CD4<sup>+</sup> T-cells in particular provides the impetus for developing new miniature devices capable of rapid capture and characterization of these cells. These cytometry microdevices most commonly employ a “panning” approach whereby the cells are captured onto Ab-decorated regions within the device, and then immunolabeled and/or enumerated (12-14). Therefore, a biological goal of the present study was to develop an approach for releasing T-cells captured inside a microdevice.

In the cell release experiments described schematically in Figure 1A, model T-lymphocytes were seeded onto a five member array of 300  $\mu\text{m}$  diameter Au electrodes connected to contact pads by 10  $\mu\text{m}$  leads. This electrode array was imbedded into a non-fouling PEG gel layer using “self-alignment” process described above. Cells were introduced onto the substrate resulting in formation of a dense, contiguous monolayer of T-cells interacting with both Au and PEG hydrogel microstructures. However, gentle aspiration of the cell seeding medium and agitation of the substrate in 1 $\times$  PBS revealed that T-cells attached exclusively on Ab-modified electrode regions with minimal cell attachment on PEG hydrogel (Figure 2C). Importantly, T-cell attachment to Au leads connecting electrodes to contact pads was eliminated by adjusting UV exposure so as to over-polymerize PEG gel around 10  $\mu\text{m}$  wide Au line.

After cell capture, a microfabricated substrate was transferred into an electrochemical cell and immersed in  $\sim$ 1 ml of 1 $\times$  PBS serving as electrolyte solution. Pt counter and Ag/AgCl reference electrodes were introduced into the electrochemical cell with T-lymphocyte capturing Au surface serving as a working electrode. Applying reductive potential (-1.2V vs. Ag/AgCl for 60 sec), followed by gentle agitation of the electrochemical cell resulted in desorption of T-lymphocytes from the electrode. Figure 2C shows an array of three gold microelectrodes employed to capture model T-cells. Upper and lower electrodes were electrically activated while a central electrode was not. As seen from this image, the electrode that was not activated contains captured T-cells, whereas activated electrodes are void of cells. These data provide additional evidence that T-cell release was due to electrode activation and was not a cell handling (e.g. shearing off) artifact. In the future, the cell sorting mechanism demonstrated here will be incorporated into a microfabricated cytometry platform for capture and interrogation of cells to enable release of specific cells based on phenotype and function determination made in the microdevice.

The paper also describes the formation of a co-culture of two cell types using electrochemical desorption of cell-resistive monolayer of PEG silane from ITO electrodes. The desorption of the molecules was carried out using ToF-SIMS by comparing mass spectra of negative secondary ions emitted from the surfaces of bare ITO, PEG silane modified ITO and PEG silane desorbed ITO. The spectrum of bare ITO on glass shown in Figure 3A, contains a characteristic indium oxide ion peak ( $m/e = 131$ ) with a yield (number of secondary ions per single projectile impact) of  $5.61 \times 10^{-3}$ . After modifying the surface with PEG silane, this characteristic peak disappears, indicating the presence of the insulating PEG silane layer (inset of Figure 3B). Significantly, applying the reductive potential to the ITO electrode resulted in the reappearance of the peak with a yield of  $5.83 \times 10^{-3}$  thus pointing to the complete removal of PEG silane from the ITO electrode (Figure 3C).

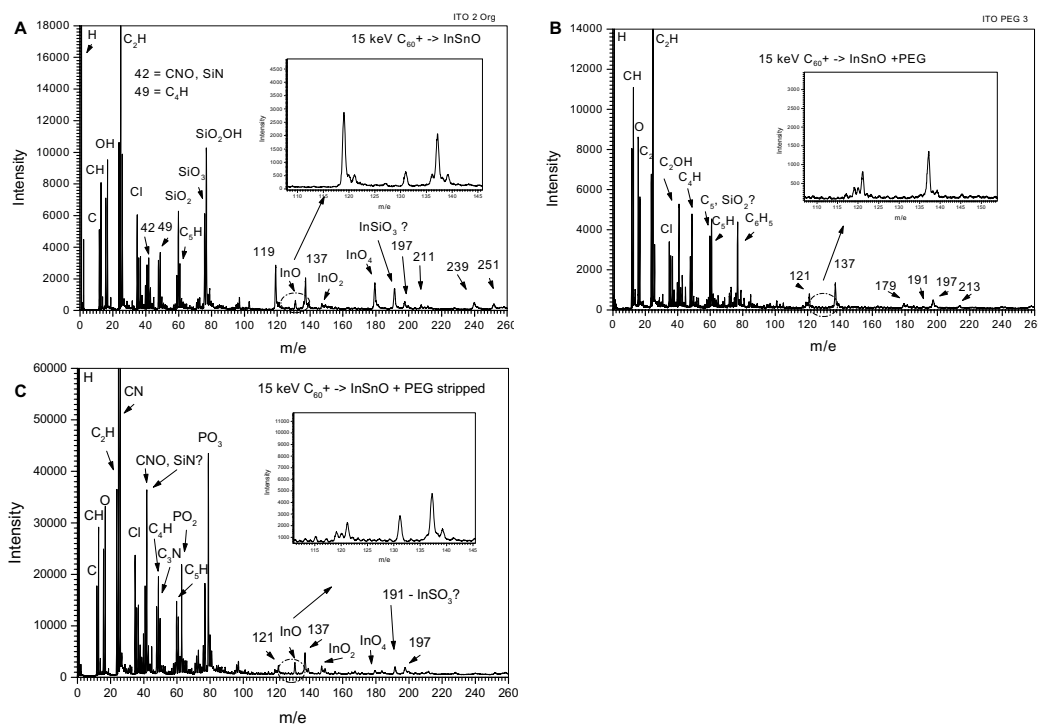


Figure 3: (A) ToF-SIMS spectrum for bare ITO substrate shows the presence of a prominent InO<sup>-</sup> peak. (B) The mass spectrum after PEG silane modification. Inset shows the disappearance of the InO<sup>-</sup> peak. (C) The mass spectrum after reductive desorption of PEG silane from ITO. Inset shows a reappearance of the InO<sup>-</sup> peak suggesting a complete removal of PEG silane from ITO. Reproduced with permission from *Langmuir* **2008**, 24, 6837-6844. Copyright 2008 American Chemical Society.

The ability to locally “switch” cell-adhesive surface properties was utilized to assemble two different types of cells on the same substrate. The process employed to create micropatterned co-cultures involved sequential activation of ITO electrodes, followed by seeding of the desired cell type. Figure 4A shows a microfabricated substrate employed for construction of co-cultures consisting of two individually addressable ITO regions modified with PEG silane. The co-culture assembly began with application of reductive potential to electrode 1 of the substrate, converting this ITO region from non-fouling to protein-adhesive. HepG2 cells were seeded after incubating the surface with collagen Type I. As seen from Figure 4B, hepatocytes exclusively attached to electrode 1 and not to electrode 2 or surrounding glass regions. After allowing hepatic cells to spread and proliferate on ITO electrode 1 for 24 h, the second ITO region was activated, causing desorption of the non-fouling PEG layer and making electrode 2 available for cell attachment. The co-culture was completed by incubating substrates containing hepatic cells and “deprotected” ITO regions with 3T3 fibroblasts to form a co-culture as seen in Figure 4C. Figure 4D highlights the presence of two cell types; the cuboidal hepatic cells residing on the ITO electrode region 1 (left side of the image) and the elongated fibroblasts adherent on the second electrode region (right side of the image).

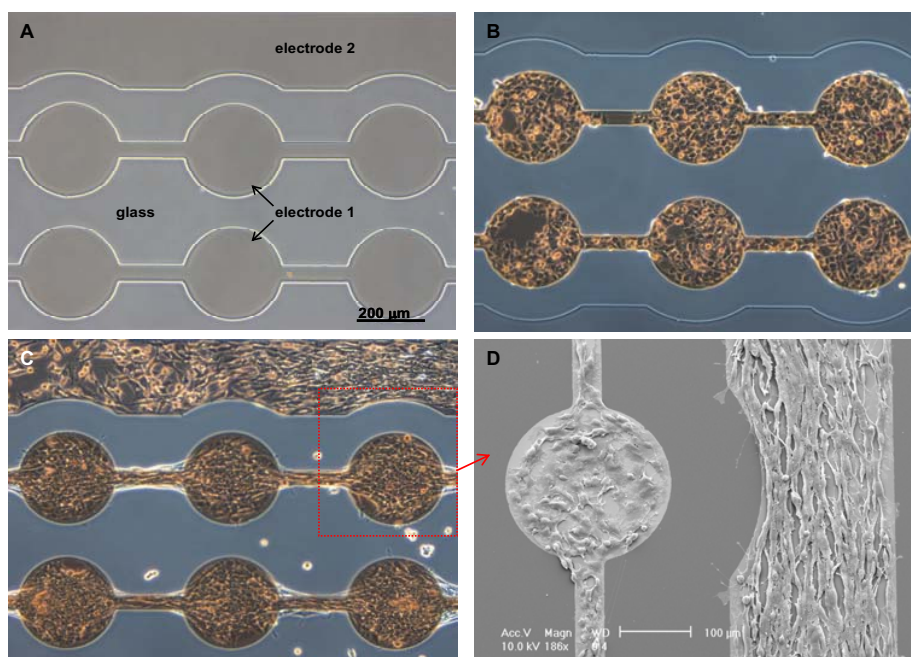


Figure 4: (A) PEG silane modification on glass substrates containing two individually addressable electrodes. (B) Desorption of PEG silane from electrode 1 followed by seeding of hepatic cells. (C) Attachment of fibroblasts after desorbing PEG silane from electrode 2 to form a co-culture. (D) SEM image showing cuboidal HepG2 cells (left side of image) and elongated fibroblasts (right side of image). Reproduced with permission from *Langmuir* **2008**, 24, 6837-6844. Copyright 2008 American Chemical Society.

### Conclusion

The ability to exercise precise spatiotemporal control over cell-surface interactions is important to the development of microdevices for diagnostic applications and multicellular constructs serving as *in vitro* mimics of native tissues. Here, we have shown a novel approach of capturing T-cells onto Ab-modified electrode arrays and then releasing cells by electrochemical desorption of the underlying Ab layer. In the future, the proposed cell-sorting approach will be employed for positive selection of specific leukocyte types from whole blood for rapid characterization and retrieval of the cells. Furthermore, we have shown micropatterning of cells on ITO electrodes by switching biointerfacial properties of the underlying non-fouling PEG silane layer. This technique may be employed to assemble multiple cell types on the same surface for tissue engineering applications.

### Acknowledgments

Financial support for this work was provided by the California Research Center for the Biology of HIV in Minorities, California HIV/AIDS Research Program #CH05-D-606 and by NIH (DK073901).



### References

1. Yousaf, M. N.; Houseman, B. T.; Mrksich, M. *Proc. Natl. Acad. Sci. USA* 98 (2001) 5992–5996.
2. W.S. Yeo, M. Mrksich, *Langmuir* 22(25) (2006) 10816–10820.
3. Jiang, X.; Ferrigno, R.; Mrksich, M.; Whitesides, G. M. *J. Am. Chem. Soc.* 125 (2003) 2366–2367.
4. Li, Y.; Yuan, B.; Ji, H.; Han, D.; Chen, S. Q.; Tian, F.; Jiang, X. Y. *Angew. Chem., Int. Ed.* 46(7) (2007) 1094–1096.
5. Tang, C. S.; Schmutz, P.; Petronis, S.; Textor, M.; Keller, B.; Voros, J. *Biotechnol. Bioeng.* 91(3) (2005) 285–295.
6. Tang, C. S.; Dusseiller, M.; Makohliso, S.; Heuschkel, M.; Sharma, S.; Keller, B.; Voros, J. *Anal. Chem.* 78(3) (2007) 711–717.
7. Zhu, H., Yan, J., and Revzin, A., *Colloids and Surfaces B: Biointerfaces* 64 (2008) 260-268.
8. S.G. Balasubramanian, A. Revzin, A.L. Simonian, *Electroanalysis* 18 (2006) 1885.
9. Shah, S., Lee, JY., Verkhoturov, S., Tuleuova, N., Schweikert, E., Ramanculov, E., and Revzin, A., *Langmuir* 24 (2008) 6837-6844.
10. R. F. Siliciano; T. Lawton; C. Knall; R. W. Karr; P. Berman; T. Gergory; E. L. Reinherz. *Cell* 54 (1988) 561-575.
11. R. S. Veazey; M. DeMaria; L. V. Chalifoux; D. E. Shvetz; D. R. Pauley; H. L. Knight; M. Rosenzweig; R. P. Johnson; R. C. Desrosiers; A. A. Lackner. *Science* 280 (1998) 427-431.
12. A. Revzin; K. Sekine; A. Sin; R. G. Tompkins; M. Toner. *Lab Chip* 5 (2005) 30-37.
13. X. H. Cheng; D. Irimia; M. Dixon; K. Sekine; U. Demirci; L. Zamir; R. G. Tompkins; W. Rodriguez; M. Toner. *Lab Chip* 7(2) (2007) 170-178.
14. K. Sekine; A. Revzin; R. G. Tompkins; M. Toner. *J. Immunol. Methods* 313 (2006) 96-109.